Gene expression profiling in the early phases of DMD: A constant molecular signature characterizes DMD muscle from early…

Article *in* The FASEB Journal · May 2007

DOI: 10.1096/fj.06-7285com · Source: PubMed

CITATIONS
114

READS
99

17 authors, including:

Mario Pescatori
Erasmus MC
86 PUBLICATIONS **1,301** CITATIONS
SEE PROFILE

Enrico Bertini
Ospedale Pediatrico Bambino Gesù
779 PUBLICATIONS **18,404** CITATIONS
SEE PROFILE

Giorgio Tasca
Catholic University of the Sacred Heart
107 PUBLICATIONS **826** CITATIONS
SEE PROFILE

Enzo Ricci
Catholic University of the Sacred Heart
215 PUBLICATIONS **5,534** CITATIONS
SEE PROFILE

Gene expression profiling in the early phases of DMD: a constant molecular signature characterizes DMD muscle from early postnatal life throughout disease progression

Mario Pescatori,[*,‡‡,1] Aldobrando Broccolini,[*] Carlo Minetti,[†] Enrico Bertini,[‡] Claudio Bruno,[†] Adele D'amico,[‡] Camilla Bernardini,[§] Massimiliano Mirabella,[*,‡‡] Gabriella Silvestri,[*] Vincenzo Giglio,[‖,††] Anna Modoni,[*] Marina Pedemonte,[†] Giorgio Tasca,[*] Giuliana Galluzzi,[††] Eugenio Mercuri,[*] Pietro A. Tonali,[*,‡‡] and Enzo Ricci[*,‡‡,1]

[*]Institute of Neurology, Catholic University, Rome, Italy; [†]Neuromuscular Disease Unit, Department of Pediatrics, G. Gaslini Institute, University of Genova, Genova, Italy; [‡]Unit of Molecular Medicine and Pathology, Bambino Gesù Children's Hospital IRCCS, Rome, Italy; [§]Institute of Anatomy and Cell Biology, Catholic University, Rome, Italy; [‖]Division of Cardiology and ICU, St. Paolo Hospital, Civitavecchia, Italy; [††]Center for Neuromuscular Diseases, UILDM, Rome, Italy; and [‡‡]Don Gnocchi Foundation, ONLUS, Rome, Italy

ABSTRACT **Genome-wide gene expression profiling of skeletal muscle from Duchenne muscular dystrophy (DMD) patients has been used to describe muscle tissue alterations in DMD children older than 5 years. By studying the expression profile of 19 patients younger than 2 years, we describe with high resolution the gene expression signature that characterizes DMD muscle during the initial or "presymptomatic" phase of the disease. We show that in the first 2 years of the disease, DMD muscle is already set to express a distinctive gene expression pattern considerably different from the one expressed by normal, age-matched muscle. This "dystrophic" molecular signature is characterized by a coordinate induction of genes involved in the inflammatory response, extracellular matrix (ECM) remodeling and muscle regeneration, and the reduced transcription of those involved in energy metabolism. Despite the lower degree of muscle dysfunction experienced, our younger patients showed abnormal expression of most of the genes reported as differentially expressed in more advanced stages of the disease. By analyzing our patients as a time series, we provide evidence that some genes, including members of three pathways involved in morphogenetic signaling—Wnt, Notch, and BMP—are progressively induced or repressed in the natural history of DMD.—Pescatori, M., Broccolini, A., Minetti, C., Bertini, E., Bruno, C., D'amico, A., Bernardini, C., Mirabella, M., Silvestri, G., Giglio, V., Modoni, A., Pedemonte, M., Tasca, G., Galluzzi, G., Mercuri, E., Tonali, P. A., Ricci, E. Gene expression profiling in the early phases of DMD: a constant molecular signature characterizes DMD muscle from early postnatal life throughout disease progression. *FASEB J.* 21, 1210–1226 (2007)**

Key Words: microarrays · Duchenne muscular dystrophy · human disease · Wnt, Notch, and BMP signaling

Duchenne muscular dystrophy (DMD) is a degenerative skeletal muscle disease caused by mutations in the dystrophin gene located on the short arm of the X chromosome (Xp21). DMD affects 1 in 3500 boys, and is characterized by the absence of detectable dystrophin protein expression on muscle fibers (1).

In mature muscle, dystrophin is localized adjacent to the cytoplasmic face of the sarcolemmal membrane in a cytoskeletal protein assembly, termed costameres, that links the force generating sarcomeric apparatus to the sarcolemmal membrane and the extracellular matrix (ECM). In this location, dystrophin is associated with a large oligomeric complex—the dystrophin-glycoprotein complex (DGC) (2)—which bridges the costameric cytoskeleton and the ECM. In the absence of dystrophin, greater stress is placed on myofibrillar and membrane proteins on muscle contraction. This produces severe muscle damage and generates a restless cycle of necrotic/regenerative dynamics. The progressive inability of DMD skeletal muscle to properly complete tissue regeneration leaves a fatty fibrous "scar," ultimately determining the muscle contractile dysfunction typical of the disease.

Albeit an increased serum creatine kinase level and abnormal muscle histology are always present, boys with DMD are phenotypically indistinguishable from the

[1]Correspondence: M.P. and E.R.: Institute of Neurology, Catholic University, L.go A. Gemelli 8, 0018, Rome, Italy. E-mail: m.pescatori@rm.unicatt.it; ericci@rm.unicatt.it

doi: 10.1096/fj.06-7285com

0892-6638/07/0021-1210 © FASEB

normal ones at birth and, in their first years of life, acquire early motor milestones at normal times. A clear defect in muscle function becomes generally apparent by the end of the second year. As the disease is typically diagnosed between the ages of 3 and 7, the first 2 years are often considered and referred to as clinically presymptomatic.

Large-scale parallel gene expression analysis of skeletal muscle biopsies from DMD patients and unaffected controls has been successfully used in some recent studies to describe at a transcriptional level shared muscle tissue alterations in DMD children older than 5 years (3–7), when the disease first shows its major consequences on muscle function and ambulation. As a defined gene expression signature was shown to characterize these symptomatic patients, we sought to investigate whether and to which extent alterations may also be present in muscle from DMD infants. To this aim, we used Affymetrix technology to compare the individual expression profiles of 19 DMD patients with age at biopsy scattered along the first 2 years of the disease with those of 14 age-matched controls. This approach allowed us to describe with high resolution the altered transcriptional state that characterizes this early, presymptomatic phase of the disease and highlight some molecular pathways as potential critical targets in the pathophysiology of the disease.

MATERIALS AND METHODS

Subjects

Relevant data about the participants are posted under "supplemental material" (Table ST1). All DMD patients (n=22) had a diagnosis of Duchenne muscular dystrophy based on the absence of dystrophin immunoreactivity on quadriceps muscle sections. None of the participants at the time of biopsy was or had been under corticosteroid treatment. Control biopsies (n=14) were from individuals who came to the hospital with a suspect metabolic disorder that was not confirmed by biochemical and histopathological studies. Control biopsies did not show signs of muscle pathology on histological and histochemical examination.

All bioptic specimens used in this study were taken, for diagnostic purposes, under institutionally approved protocols. Since all our patients were minors, their parents were asked to sign an informed consent disclosing future use of the bioptic materials for research. This study was reviewed and authorized by our institutional Ethics Committee, according to our institutional regulation and national laws and guidelines.

RNA extraction

Total RNA was extracted from frozen quadriceps muscle biopsies by TriZol (TriZol reagent, Invitrogen, Carlsbad, CA, USA). RNA was further purified using the RNAeasy mini kit following the RNA cleanup protocol as indicated by the manufacturer (Qiagen, Valencia, CA, USA). RNA purity and integrity were assessed by spectophotometric analysis and agarose gel electrophoresis.

Affymetrix GeneChips

We use one type of gene chip in this study: the Affymetrix HG-U133A GeneChip. CRNA synthesis was performed using 5 μg of total RNA as template, as described in the Affymetrix *Gene Expression Manual*. Gene chips were washed and stained in an Affymetrix fluidic station 430 and analyzed on an Affymetrix G2500 GeneChip scanner. To prevent overcorrelation, samples were processed eight at a time and arranged so that DMD and control samples were both in each experimental session.

Data analysis

Data analysis was performed using BRB ArrayTools developed by Dr. Richard Simon and Amy Peng Lam (8–10).

Probe level summaries were generated using an empirically motivated statistical approach: the log scale robust multiarray analysis (rma) procedure developed by Irizzarry *et al.* (11). An expression table reporting normalized, background corrected, probe level summaries for all the 22,283 probesets is posted under supplemental material (DMDDATA_rma). The data set was filtered to exclude from the analysis genes showing minimal variation across the set of arrays. Probesets whose expression differed by at least 1.5-fold from the median in at least 20% of the arrays were retained.

All the experiments in this work met specific GeneChip QC criteria (supplemental material, GeneChip QC). A data table (rma), together with the relative cel files and relevant information about the experiment, is available at http://www.ncbi.nlm.nih.gov/geo/ under accession #GSE6011. Whenever needed, association probability (P value) and correlation coefficient (R^2) among genes or samples were computed using Excel.

Multidimensional scaling (MDS)

Multidimensional scaling is a group of methods for representing high-dimensional data graphically in low (usually 2 or 3) dimensions. The objective in multidimensional scaling is to preserve pairwise similarities or distances between objects in the low-dimensional graphical representation. Multidimensional scaling analysis is similar to cluster analysis in that one is attempting to examine relationships among samples, but it also provides a graphical representation of the pairwise similarities or distances among samples without forcing the samples into specific clusters. We measured the similarity between gene expression patterns by computing the correlation distances (1-Pearson correlation) for each pair of samples based on standardized log-transformed expression values across all of the genes passing the general filtering (see Data analysis). During the multidimensional scaling procedure (BRB ArrayTools, Multidimensional scaling), samples were positioned in a 3-dimensional space so that the distance between each pair of samples very closely approximated the correlation distance measurements in the matrix for the corresponding sample pair (8–10). Samples with gene expression profiles more similar to each other will lie closer and form an aggregation (cluster) in 3-dimensional space. We also ran the same analysis using Euclidean distances, and the result was similar, showing separate clustering of DMD and control samples

Class comparison

We computed the probability of genes being differentially expressed between the two classes, using the unequal variance t test, and identified genes differentially expressed between

the two classes by a multivariate permutation test (8–10) to provide 95% confidence that the false discovery rate was <10% (BRB ArrayTools, Class comparison). Although *t* statistics were used, the multivariate permutation test is nonparametric and does not require the assumption of Gaussian distributions. The results of this analysis are displayed as an html file reporting all the differentially expressed genes ranked by *P* value and tabulated along with descriptive statistics and links to the Entrez/gene database (supplemental material, DMDCLASSCOMP_filt).

Gene ontology

The evaluation of which gene ontology classes were differentially expressed between normal and DMD samples was performed using a functional class scoring analysis as described by Pavlidis *et al.* (12). For each gene in a GO class, the *P* value for comparing normal *vs.* DMD samples was computed. The set of *P* values for a class was summarized by two summary statistics: *1)* the LS summary is the average log *P* values for the genes in that class and *2)* the KS summary is the Kolmogorov-Smirnov statistic computed on the *P* values for the genes in that class. The statistical significance of the GO class containing *n* genes represented on the array was evaluated by computing the empirical distribution of these summary statistics in random samples of n genes. We considered a GO category differentially regulated if the significance level of either one of the KS or LS statistics was <0.005 (BRB ArrayTools, Class comparison). The results of this analysis are displayed as an html file (Supplemental Material, DMDGO).

Correlation analysis

To search for genes whose expression was significantly related to patient age, we computed the significance level for each gene to test the hypothesis that the Spearman's correlation between gene expression and age was zero. These *P* values were then used in a multivariate permutation test (8–10) in which ages were randomly permuted among arrays to provide confidence that the median value of false discoveries was <10 (BRB ArrayTools, Quantitative Trait Analysis). The multivariate permutation test is nonparametric and does not require the assumption of Gaussian distributions.

Patients were arbitrarily grouped into 4 age defined classes:
Class 1: 1.5–5 months, $n = 5$
Class 2: 6–12 months, $n = 8$
Class 3: 14–22 months, $n = 6$
Class 4: 28–61 months, $n = 3$

The results of the analysis are displayed as an html file reporting correlated genes ranked by *P* value and tabulated along with descriptive statistics and links to the Entrez/gene database (supplemental material, DMDAGECORR). We ran a similar correlation analysis across all the control profiles. None of the genes showing age dependence in patients showed a similar behavior in controls. To exclude the possibility that genes presented as modulated with age in patients and those discussed in this article were regulated similarly in controls, we browsed the data set and analyzed the trends of expression in controls for the 16 genes reported in Table 3. This was done by plotting the absolute expression values of the control subjects, ordered by increasing age, and visually inspecting the expression trends, highlighted by the resulting curve. Using this procedure, we identified three genes (MAPRE3, C6orf106, and POSTN) whose expression showed age dependence in both patients and controls.

We are aware that the particular grouping chosen is arbitrary and that changing the number, size, and composition of the classes would affect results of the analysis. The number of genes reported is small and likely represents a gross underestimation of the real number of those modulated along the progression of the DMD. This approach therefore was not intended to provide a comprehensive description of the progression of the disease; it was a tool that allowed us to identify some genes whose expression trends, in our patients, might suggest a role in progressive pathophysiological processes.

Pathogenic components analysis

We defined four clusters of genes as representative of four major aspects of DMD pathophysiology (muscle regeneration/immaturity, inflammation, ECM homeostasis, and energy metabolism). From the class comparison results, we sorted genes involved in the relevant pathophysiological processes into four lists based on information obtained from both public databases (NCBI Entrez Gene, Jackson Laboratory Mouse Genome Informatics and Weitzman Institute of Science Gene Cardsl) and upon extensive search of the scientific literature in PubMed. The four lists were made nonredundant (one probeset for gene), and gene clustering (BRB ArrayTools, 2-way clustering algorithm, average linkage, "one minus correlation" distance, median-centered expression values) was used to extract from each list a correlated component showing covariation of the expression values across the data set. For each gene, log2 expression values were expressed as the ratio to the mean of the control population. The resulting fold changes were averaged in each cluster to generate four indexes (average log2 fold change in cluster) we consider indicative of the extent of activation of these four aspects of the disease.

Real-time rt-PCR

Two-step, real-time polymerase chain reaction (PCR) reactions were performed on skeletal muscle RNA from 15 DMD patients (DMD1, DMD2, DMD3, DMD4, DMD5, DMD7, DMD9, DMD11, DMD12, DMD13, DMD15, DMD18, DMD19, DMD21, and DMD22) and 8 unaffected controls (C1, C3, C4, C7, C9, C11, C12, and C13). First-strand cDNA was synthesized from 1 μg total RNA using Superscript II (Life Technologies, Carlsbad, CA, USA) and an oligo dT primer, following the manufacturer's instructions. Real-time PCR was performed on an ABI Prism 7000 Sequence Detection System using the Applied Biosystem TaqMan universal PCR master mix (with UNG) and the following gene-specific TaqMan primers sets (Applied Biosystems, Foster City, CA, USA): GAPDH, Hs99999905_m1; MCSP/NG2, Hs00426981_m1; MYH3, Hs00159463_m1; MYH8, Hs00267293_m1; ACTC, Hs00606316_m1; CHRNA1, Hs00175578_m1; COL3A1, Hs00164103_m1; COL1A1, Hs00164004_m1; COL1A2, Hs00164099_m1; CALP6, Hs00560073_m1; CHRNG, Hs00183228_m1; CHRNE, Hs00181084_m1; myostatin, Hs00193363_m1; follistatin, Hs00246260_m1; FSTL1, Hs00200053_m1. Standard curves were generated to verify PCR efficiency. After amplification, the difference between threshold cycles Δct (ct GeneX-ct GAPDH) was calculated for all samples and the mean Δct value in the control population was subtracted from all samples. Log2 expression differences were converted to fold change ratios using the equation $FC = 2^{-\Delta ct}$. The unequal variance *t* test was used to compute the probability of genes being differentially expressed between the two classes (Excel).

RESULTS

Normal and DMD skeletal muscles display different gene expression patterns

We found a strong distinction in the genome-wide pattern of gene expression between normal and DMD muscle (**Fig. 1**). This result indicates that the large set of differentially expressed genes makes it possible to draw a line between normal and DMD skeletal muscle based solely on the overall similarity of gene expression patterns.

DMD *vs.* control class comparison: genes and gene ontology (GO) categories modulated in DMD skeletal muscle

Of the 22283 probe sets represented on the HG U133A GeneChip, 1663 (7.5%) met inclusion criteria and were retained for further analysis. As a result of the *t* test, 127 probe sets were differentially expressed between the two classes with a *P* value lower than 1E-07, 202 with $P <$ 1E-06, 281 with $P <$ 1E-05, 399 with $P <$ 1E-04, and 561 with $P <$ 1E-03. To control the proportion of false discoveries within differentially expressed genes, we used a multivariate permutation test to provide the 95% confidence that the false discovery rate was <10% (8–10). By this cutoff statistic, we identified 777 probe sets as differentially expressed; this was equivalent to applying a probability threshold of 9.7E-03. A table reporting a list of these probe sets, ranked by *P* value and tabulated along with within-class geometric mean, between-classes fold difference, and annotations, is posted under supplemental material (DMDCLASSCOMP_filt). Since many genes are represented on the U133A GeneChip by multiple probes, these 777 probe sets are representative of 618 genes. Among them, more are overexpressed (421/618) than underexpressed (197/618). **Table 1** reports a selection of differentially expressed genes grouped by function. We should mention that the fold change estimates generated by our analysis are smaller than those reported earlier by other authors (3–7). The difference can be attributed to the use of a different probe set summarization algorithm, rma, which is more precise than MAS5.0 but produces lower fold change estimates (11). The possibility that this discrepancy is due to the different ages of the patients studied can be ruled out, as we included in our study two older patients (aged 4 and 5 years) who showed expression values and fold changes comparable to presymptomatic patients.

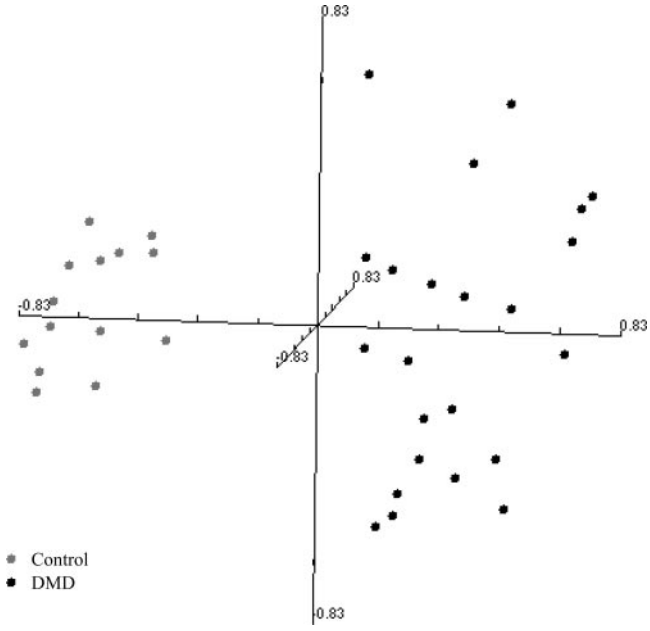

Figure 1. Unsupervised multidimensional scaling (MDS) of the expression profiles from quadriceps muscle biopsies showing separate clustering of DMD and control samples. The high dimensionality of the gene expression data has been reduced to the 3 dimensions that comprise the greatest variation across the data set. Skeletal muscle samples are represented by spheres and positioned in the 3-dimensional space, so that the distance between each pair of samples very closely approximates the "one minus correlation" (centered) distance for the corresponding sample pair. A clear separation between DMD (black) and control (gray) samples is achieved along one of the three components of the plot, with DMD samples showing greater spreading than controls.

Fourteen genes showed in all patients expression values greater than the greatest value observed in controls; conversely, no genes had in all patients expression values lower than the lowest in controls (**Table 2**). The two genes more frequently underexpressed, outside the control range in 21/22 patients, were the muscle-type glycogen phosphorylase (PYGM) and CAPRI, a Ca^{2+}-dependent, RAS GTPase-activating protein (AP) (RASA4) that interacts with members of the RHO and CDC42 family of small G-proteins. Dystrophin mRNA was reduced in 20 of 22 patients.

Complementary to the gene-based approach, we provided additional information by evaluating which gene ontology classes were differentially expressed between normal and DMD muscle (10, 12). A table reporting results of the analysis is posted under supplemental material (DMDGO).

Transcriptome alteration in DMD skeletal muscle

Muscle genes

The group of genes showing the greatest changes in expression encodes myofibrillar components induced along with the activation of a *bona fide* muscle regeneration program. This includes postnatal re-expression of developmental isoforms of sarcomeric proteins and increased transcription of genes encoding postsynaptic NMJ components and cytoskeletal elements supporting chronic remodeling of sarcomeric structures (13). By real-time PCR, we also detected induction of the nAChR gamma subunit (CHRNG), whose expression is shut down at birth and replaced by the postnatal-type epsilon subunit (CHRNE) in normal individuals (14, 15) (supplemental material, Table ST2). More than 40

TABLE 1. *Differentially expressed genes grouped into three major categories: muscle genes, inflammation,* and *ECM remodeling*[a]

Gene symbol	Gene name	Probe set	Fold change	*P* value
Muscle genes				
MLC1SA	Myosin light chain 1 slow type	204173_at	1.65	1.61E-03
MYBPC2	Myosin binding protein C, fast type	206394_at	0.65	3.84E-03
MYBPH	Myosin binding protein H	206304_at	3.95	$P < 1e-07$
MYH3	Myosin, heavy polypeptide 3, embryonic	205940_at	23.81	$P < 1e-07$
MYH8	Myosin, heavy polypeptide 8, perinatal	206717_at	19.23	$P < 1e-07$
MYL4	Myosin, light polypeptide 4, alkali; embryonic	210395_x_at	2.15	$P < 1e-07$
MYL5	Myosin, light polypeptide 5, regulatory	205145_s_at	3.14	3.00E-07
MYL6	Myosin, light polypeptide 6, alkali	212082_s_at	2.09	1.30E-06
MYL9	Myosin, light polypeptide 9, regulatory	201058_s_at	1.52	8.95E-03
ACTC	Actin, alpha, cardiac muscle	205132_at	6.99	$P < 1e-07$
TNNT2	Troponin T2, cardiac	215389_s_at	2.92	$P < 1e-07$
CHRNA1	Cholinergic receptor, nicotinic, alpha 1	206633_at	3.29	$P < 1e-07$
RYR1	Ryanodine receptor 1	205485_at	0.65	2.97E-05
LMOD1	Leiomodin 1	203766_s_at	0.55	8.00E-07
PLN	Phospholamban	204940_at	0.59	1.57E-03
CALR	Calreticulin	214315_x_at	1.41	5.95E-03
CALD1	Caldesmon 1	212077_at	1.63	1.31E-03
ACTB	Actin, beta	213867_x_at	1.74	$P < 1e-07$
ACTG1	Actin, gamma 1	201550_x_at	1.87	1.00E-07
ACTN1	Actinin, alpha 1	208636_at	1.94	7.20E-06
ACTN2	Actinin, alpha 2	203863_at	0.66	6.26E-04
ACTR2	ARP2 actin-related protein 2 homolog	200728_at	1.45	1.15E-03
ACTR3	ARP3 actin-related protein 3 homolog	213101_s_at	1.75	4.70E-05
ARPC1B	Actin-related protein 2/3 complex, subunit 1B 41 kDa	201954_at	1.74	2.00E-06
ARPC3	Actin-related protein 2/3 complex, subunit 3, 21 kDa	208736_at	1.72	7.73E-05
K-ALPHA-1	Tubulin, alpha, ubiquitous	212639_x_at	2.06	$P < 1e-07$
TUBA3	Tubulin, alpha 3	209118_s_at	3.40	$P < 1e-07$
TUBA6	Tubulin alpha 6	209251_x_at	1.85	$P < 1e-07$
TUBB	Tubulin, beta polypeptide	204141_at	2.38	9.89E-05
TUBB2	Tubulin, beta, 2	213726_x_at	1.46	1.41E-03
TUBB4	Tubulin, beta, 4	213476_x_at	1.78	1.04E-05
TUBB6	Tubulin beta 6	209191_at	4.18	$P < 1e-07$
MACF1	Microtubule-actin cross-linking factor 1	208634_s_at	1.53	1.83E-05
CKAP1	Cytoskeleton-associated protein 1	216194_s_at	1.61	1.92E-04
CKAP4	Cytoskeleton-associated protein 4	200999_s_at	1.80	8.04E-05
CNN3	Calponin 3, acidic	201445_at	1.76	7.90E-05
NES	Nestin	218678_at	2.60	$P < 1e-07$
VIM	Vimentin	201426_s_at	2.09	2.78E-05
PLEC1	Plectin 1, intermediate filament binding prot 500 kDa	216971_s_at	0.65	2.69E-03
SVIL	Supervillin	202566_s_at	0.72	3.61E-03
NRAP	Nebulin-related anchoring protein	207089_at	0.50	8.25E-03
FHL3	Four and a half LIM domains 3	218818_at	0.55	1.07E-05
RSN	Restin (intermediate filament-associated protein)	210716_s_at	0.69	2.86E-04
DMD	Dystrophin	203881_s_at	0.18	$P < 1e-07$
FER1L3	fer-1-like 3 (myoferlin)	201798_s_at	2.40	$P < 1e-07$
SGCE	Sarcoglycan, epsilon	204688_at	1.55	1.07E-03
SNTA1	Syntrophin, alpha 1	203516_at	0.70	4.26E-04
HOMER1	Homer homolog 1	213793_s_at	1.48	2.84E-03
FKBP1A	FK506 binding protein 1A	200709_at	1.54	2.96E-04
CD9	CD9 antigen (p24)	201005_at	1.71	1.01E-04
AQP4	Aquaporin 4	210068_s_at	0.60	1.38E-04
KCNJ12	Potassium inwardly rectifying channel, J12	207110_at	0.75	4.35E-03
KCNJ2	Potassium inwardly rectifying channel, J2	206765_at	0.70	5.07E-03
KCTD12	Potassium channel tetramerization domain 12	212192_at	2.29	7.57E-05
SCN1B	Sodium channel, voltage-gated, type I, beta	205508_at	0.61	1.00E-07
VDAC1	Voltage-dependent anion channel 1	217140_s_at	0.55	5.78E-05
CACNA1S	Calcium channel, voltage-dependent, L type alpha 1	217515_s_at	0.69	7.97E-04
MYOD1*	Myogenic factor 3	206657_s_at	1.22	1.50E-02
MYOG	Myogenin (myogenic factor 4)	207282_s_at	1.62	4.10E-06
MEF2C	MADS box transcription enhancer factor 2, C	209200_at	1.52	5.96E-04
CCNG2	Cyclin G2	202769_at	1.58	2.36E-04
CCND2	Cyclin D2	200953_s_at	1.82	$P < 1e-07$
CDK4*	Cyclin-dependent kinase 4	202246_s_at	1.21	2.99E-03
CDKN1A	Cyclin-dependent kinase inhibitor 1A (p21, Cip1)	202284_s_at	1.84	2.04E-04

Continued on next page

TABLE 1. (*continued*)

Gene symbol	Gene name	Probe set	Fold change	*P* value
GADD45A	Growth arrest and DNA damage-inducible, alpha	203725_at	1.81	3.87E-04
IGF1	Insulin-like growth factor 1 (somatomedin C)	209541_at	1.73	8.43E-03
IGF2	Insulin-like growth factor 2 (somatomedin A)	202409_at	1.78	7.65E-04
IGFBP4	Insulin-like growth factor binding protein 4	201508_at	1.81	9.20E-06
IGFBP7	Insulin-like growth factor binding protein 7	201162_at	1.80	2.14E-05
PRSS11*	Protease, serine, 11 (IGF binding)	201185_at	1.63	9.00E-8
CKB	Creatine kinase, brain	200884_at	1.51	1.58E-03
GAMT	Guanidinoacetate N-methyltransferase	205354_at	0.69	2.71E-03
PYGM	Phosphorylase, glycogen; muscle	205577_at	0.56	5.00E-07
PHKA1	Phosphorylase kinase, alpha 1 (muscle)	205450_at	0.59	3.00E-07
PHKG1	Phosphorylase kinase, gamma 1 (muscle)	207312_at	0.69	2.02E-03
GYG	Glycogenin	201554_x_at	0.71	4.05E-03
PFKM	Phosphofructokinase, muscle	210976_s_at	0.70	4.58E-04
PGM1	Phosphoglucomutase 1	201968_s_at	0.59	1.59E-05
PGAM1	Phosphoglycerate mutase 1 (brain)	200886_s_at	1.63	1.02E-05
PGAM2	Phosphoglycerate mutase 2 (muscle)	205736_at	0.60	3.49E-04
OGDH	oxoglutarate dehydrogenase	201282_at	0.71	1.05E-03
ENO1	Enolase 1 (alpha)	201231_s_at	1.70	6.60E-06
ENO3	Enolase 3 (beta, muscle)	204483_at	0.64	1.33E-05
DLAT	Dihydrolipoamide S-acetyltransferase	213149_at	0.69	6.55E-03
PDK2	Pyruvate dehydrogenase kinase	202590_s_at	0.68	7.66E-05
SUCLG1	Succinate-CoA ligase, GDP-forming, alpha subunit	217874_at	0.77	9.05E-03
SUCLG2	Succinate-CoA ligase, GDP-forming, beta subunit	212459_x_at	0.66	1.72E-03
ACO2	Aconitase 2, mitochondrial	200793_s_at	0.65	1.01E-04
IDH3A	Isocitrate dehydrogenase 3 (NAD+) alpha	202069_s_at	0.68	6.71E-04
FBP2	fructose-1,6-bisphosphatase 2	206844_at	0.52	2.48E-04
GPD1	Glycerol-3-phosphate dehydrogenase 1	204997_at	0.63	1.88E-04
GPD1L	Glycerol-3-phosphate dehydrogenase 1-like	212510_at	0.54	7.00E-07
PFKFB3	6-Phosphofructo-2-kinase	202464_s_at	0.36	1.58E-04
ALDH2	Aldehyde dehydrogenase 2 family (mitochondrial)	201425_at	0.52	1.70E-06
DCXR	Dicarbonyl/L-xylulose reductase	217973_at	0.58	6.43E-05
TKT	Transketolase	208700_s_at	1.45	1.31E-03
ACSL1	acyl-CoA synthetase long-chain family member 1	207275_s_at	0.62	1.04E-04
ACADM	acyl-Coenzyme A dehydrogenase	202502_at	0.62	2.21E-04
ACADVL	acyl-Coenzyme A dehydrogenase	200710_at	0.64	1.31E-03
HADHA	hydroxyacyl-Coenzyme A dehydrogenase	208631_s_at	0.70	2.36E-03
HADHB	hydroxyacyl-Coenzyme A dehydrogenase	201007_at	0.58	3.40E-06
LPIN1	Lipin 1	212276_at	0.49	6.00E-07
LPL	Lipoprotein lipase	203548_s_at	0.40	5.24E-04
DCI	Dodecenoyl-coenzyme A delta isomerase	209759_s_at	0.73	7.69E-03
MLYCD	Malonyl-CoA decarboxylase	218869_at	0.62	2.89E-05
ACAT1	acetyl-Coenzyme A acetyltransferase 1	205412_at	0.60	1.30E-05
HMGCS2	3-Hydroxy-3-methylglutaryl-coenzyme A synthase 2	204607_at	0.42	9.12E-04
NDUFS7	NADH dehydrogenase (ubiquinone) Fe-S protein 7	211752_s_at	0.62	4.07E-03
CYC1	Cytochrome *c*-1	201066_at	0.72	3.48E-03
ETFDH	Electron-transferring flavoprotein dehydrogenase	205530_at	0.66	7.09E-04
COX6A1	Cytochrome *c* oxidase subunit VIa polypeptide 1	200925_at	1.58	5.22E-04
UCP2	Uncoupling protein 2 (mitochondrial, proton carrier)	208998_at	2.11	$P <$ 1e-07
UCP3	Uncoupling protein 3 (mitochondrial, proton carrier)	207349_s_at	0.39	1.23E-04
SLC25A11	Solute carrier family 25 member 11	207088_s_at	0.73	4.32E-03
SLC25A12	Solute carrier family 25 member 12	203340_s_at	0.74	7.95E-03
SLC25A4	Solute carrier family 25 member 4	202825_at	0.64	7.23E-05
SLC25A6	Solute carrier family 25 member 6	212085_at	1.74	2.57E-05
SLC39A6	Solute carrier family 39 member 6	202088_at	1.42	7.09E-04
ALDH5A1	Aldehyde dehydrogenase 5 family, member A1	203608_at	0.69	9.40E-03
ALDH6A1	Aldehyde dehydrogenase 6 family, member A1	204290_s_at	0.69	1.17E-03
CA2	Carbonic anhydrase II	209301_at	0.61	8.00E-06
GOT1	Glutamic-oxaloacetic transaminase 1	208813_at	0.56	2.17E-04
IRS2	Insulin receptor substrate 2	209185_s_at	0.72	6.97E-03
PHYH	Phytanoyl-CoA hydroxylase	203335_at	0.59	1.03E-05
OXCT1	3-Oxoacid CoA transferase 1	202780_at	1.45	1.62E-03
CPT1B	Carnitine palmitoyltransferase 1B (muscle)	210070_s_at	0.69	2.91E-03
FABP3	Fatty acid binding protein 3	214285_at	0.65	2.13E-03
ZAP128	Peroxisomal long-chain acyl-coA thioesterase	202982_s_at	0.68	2.56E-03
MAOB	Monoamine oxidase B	204041_at	0.57	$P <$ 1e-07
PHYH	Phytanoyl-CoA hydroxylase	203335_at	0.59	1.03E-05

Continued on next page

TABLE 1. (*continued*)

Gene symbol	Gene name	Probe set	Fold change	*P* value
Inflammation				
B2M	Beta-2-microglobulin class I MHC invariant chain	216231_s_at	1.69	4.34E-05
HLA-A	Major histocompatibility complex, class I, A	215313_x_at	1.83	5.44E-05
HLA-B	Major histocompatibility complex, class I, B	209140_x_at	1.82	2.34E-05
HLA-C	Major histocompatibility complex, class I, C	208812_x_at	1.70	5.03E-05
HLA-E	Major histocompatibility complex, class I, E	200905_x_at	1.46	2.55E-04
HLA-F	Major histocompatibility complex, class I, F	204806_x_at	1.52	2.62E-04
HLA-G	Major histocompatibility antigen, class I, G	211528_x_at	1.41	8.94E-04
CD74	CD74 antigen, class II MHC invariant chain	209619_at	2.52	$P <$ 1e-07
HLA-DMA	Major histocompatibility complex, class II, DMα	217478_s_at	2.39	$P <$ 1e-07
HLA-DPA1	Major histocompatibility complex, class II, DPα1	211990_at	3.51	$P <$ 1e-07
HLA-DPB1	Major histocompatibility complex, class II, DPβ1	201137_s_at	2.82	$P <$ 1e-07
HLA-DQA1	Major histocompatibility complex, class II, DQα1	212671_s_at	2.27	9.00E-07
HLA-DQB1	Major histocompatibility complex, class II, DQβ1	209823_x_at	2.04	7.00E-07
HLA-DRA	Major histocompatibility complex, class II, DR α	210982_s_at	3.24	$P <$ 1e-07
HLA-DRB1	Major histocompatibility complex, class II, DRβ1	209312_x_at	2.82	$P <$ 1e-07
HLA-DRB3	Major histocompatibility complex, class II, DRβ3	215193_x_at	2.87	$P <$ 1e-07
C1QA	Complement component 1, q subcomponent, alpha	218232_at	3.12	$P <$ 1e-07
C1QB	Complement component 1, q subcomponent, beta	202953_at	2.16	$P <$ 1e-07
C1R	Complement component 1, r subcomponent	212067_s_at	2.65	$P <$ 1e-07
C1S	Complement component 1, s subcomponent	208747_s_at	2.29	$P <$ 1e-07
C3	Complement component 3	217767_at	3.69	$P <$ 1e-07
C4A	Complement component 4A	214428_x_at	0.68	1.00E-07
CFH	Complement factor H	213800_at	1.88	4.70E-06
CFHL1	Complement factor H-related 1	215388_s_at	2.29	$P <$ 1e-07
F13A1	Coagulation factor XIII, A1 polypeptide	203305_at	1.60	8.00E-07
SERPING1	Serine (or cysteine) proteinase inhibitor 1, clade G	200986_at	2.07	4.00E-07
IRF7	Interferon regulatory factor 7	208436_s_at	1.41	1.43E-03
G1P2	Interferon, alpha-inducible protein (clone IFI-15K)	205483_s_at	2.14	4.14E-03
G1P3	Interferon, alpha-inducible protein (clone IFI-6–16)	204415_at	2.15	1.27E-05
IFI16	Interferon, gamma-inducible protein 16	208966_x_at	2.64	$P <$ 1e-07
IFI44	Interferon-induced protein 44	214453_s_at	1.65	5.89E-04
IFITM1	Interferon-induced transmembrane protein 1	201601_x_at	1.76	4.00E-07
IFITM2	Interferon-induced transmembrane protein 2	201315_x_at	1.66	3.70E-06
IFITM3	Interferon-induced transmembrane protein 3	212203_x_at	1.72	1.20E-06
IFIT1	Interferon-induced with tetratricopeptide repeats 1	203153_at	1.44	8.59E-03
PLSCR4	Phospholipid scramblase 4	218901_at	1.42	6.61E-04
ADAR	Ddenosine deaminase, RNA-specific	201786_s_at	1.47	2.28E-05
CCL14	Chemokine (C-C motif) ligand 14	205392_s_at	1.34	8.37E-03
CCL2*	Chemokine (C-C motif) ligand 2	216598_s_at	1.41	1.25E-04
CXCL12	Chemokine (C-X-C motif) ligand 12	209687_at	2.33	1.00E-07
CXCL14	Chemokine (C-X-C motif) ligand 14	218002_s_at	2.10	1.16E-03
CKLFSF6	Chemokine-like factor super family 6	217947_at	1.95	4.00E-07
IL13RA1	Interleukin 13 receptor, alpha 1	201887_at	1.41	4.46E-04
CSF1R	Colony-stimulating factor 1 receptor,	203104_at	1.96	$P <$ 1e-07
APOC1	Apolipoprotein C-I	204416_x_at	1.88	2.30E-06
ITGB2	Integrin, beta 2 (mac-1 beta subunit)	202803_s_at	1.90	3.00E-07
MIF	Macrophage migration inhibitory factor	217871_s_at	1.72	1.90E-06
CD14	CD14 antigen	201743_at	2.99	$P <$ 1e-07
CD163	CD163 antigen	215049_x_at	2.15	$P <$ 1e-07
LGALS3BP	Lectin, galactoside binding, soluble, 3 binding protein	200923_at	2.02	1.00E-07
MRC1	Mannose receptor, C type 1	204438_at	2.22	$P <$ 1e-07
LY96	Lymphocyte antigen 96	206584_at	1.84	$P <$ 1e-07
LGMN	Legumain	201212_at	2.28	$P <$ 1e-07
LILRB1	Leukocyte immunoglobulin-like receptor B 1	213975_s_at	3.57	$P <$ 1e-07
CLECSF2	C-type lectin, superfamily member 2	209732_at	1.48	1.96E-05
D2S448	Melanoma-associated gene	212012_at	1.62	7.17E-05
THY1	Thy-1 cell surface antigen	213869_x_at	1.57	7.40E-06
CD99	CD99 antigen	201029_s_at	2.01	$P <$ 1e-07
CD63	CD63 antigen	200663_at	1.63	2.00E-07
CD44	CD44 antigen	212063_at	2.66	$P <$ 1e-07
COLEC12	Collectin subfamily member 12	221019_s_at	1.68	1.00E-07
TPSAB1	Tryptase beta 1	207134_x_at	1.57	5.81E-05
PLA2G2A	Phospholipase A2, group IIA	203649_s_at	3.34	1.07E-05
ANXA2	Annexin A2	201590_x_at	2.38	$P <$ 1e-07
ANXA2P2	Annexin A2 pseudogene 2	208816_x_at	1.68	$P <$ 1e-07

Continued on next page

TABLE 1. (*continued*)

Gene symbol	Gene name	Probe set	Fold change	*P* value
ANXA5	Annexin A5	200782_at	1.78	3.10E-06
ANXA1	Annexin A1	201012_at	2.16	2.00E-07
VCAM1	Vascular cell adhesion molecule 1	203868_s_at	1.96	$P <$ 1e-07
S100A10	S100 calcium binding protein A10	200872_at	2.46	$P <$ 1e-07
TLR7*	Toll-like receptor 7	220146_at	1.1	2.04E-03
ECM remodeling				
COL1A1	Collagen, type I, alpha 1	202310_s_at	4.27	$P <$ 1e-07
COL1A2	Collagen, type I, alpha 2	202404_s_at	5.13	$P <$ 1e-07
COL3A1	Collagen, type III, alpha 1	211161_s_at	4.22	$P <$ 1e-07
COL4A1	Collagen, type IV, alpha 1	211980_at	1.56	7.12E-03
COL4A2	Collagen, type IV, alpha 2	211964_at	1.61	6.34E-03
COL4A3	Collagen, type IV, alpha 3	214641_at	0.70	1.70E-03
COL5A1	Collagen, type V, alpha 1	212489_at	2.17	2.50E-06
COL5A2	Collagen, type V, alpha 2	221729_at	3.75	$P <$ 1e-07
COL6A1	Collagen, type VI, alpha 1	213428_s_at	1.93	4.00E-07
COL6A2	Collagen, type VI, alpha 2	209156_s_at	2.21	2.90E-06
COL6A3	Collagen, type VI, alpha 3	201438_at	2.47	$P <$ 1e-07
COL14A1	Collagen, type XIV, alpha 1 (undulin)	212865_s_at	1.54	2.85E-04
COL15A1	Collagen, type XV, alpha 1	203477_at	1.53	6.71E-03
COL18A1	Collagen, type XVIII, alpha 1	209082_s_at	1.32	9.53E-03
FN1	Fibronectin 1	216442_x_at	1.71	2.00E-04
LAMA2	Laminin, alpha 2 (merosin)	205116_at	1.43	2.59E-03
LAMA4	Laminin, alpha 4	202202_s_at	1.69	5.48E-04
LAMB1	Laminin, beta 1	201505_at	1.60	2.87E-03
LAMB2	Laminin, beta 2 (laminin S)	216264_s_at	1.53	5.80E-05
LUM	Lumican	201744_s_at	5.03	$P <$ 1e-07
DCN	Decorin	211896_s_at	2.07	$P <$ 1e-07
BGN	Biglycan	201261_x_at	1.78	1.00E-07
ASPN	Asporin (LRR class 1)	219087_at	4.33	$P <$ 1e-07
ELN	Elastin	212670_at	1.95	7.50E-06
CSPG2	Chondroitin sulfate proteoglycan 2 (versican)	204620_s_at	2.96	$P <$ 1e-07
SDC2	Syndecan 2 (heparan sulfate proteoglycan 1)	212158_at	1.48	9.56E-04
SPARC	Secreted protein, acidic, cysteine-rich (osteonectin)	200665_s_at	2.41	1.00E-07
NID2	Nidogen 2 (osteonidogen)	204114_at	1.79	6.52E-05
DPT	Dermatopontin	213068_at	1.97	8.00E-05
EFEMP1	EGF-containing fibulin-like ECM protein 1	201842_s_at	2.37	2.00E-06
EFEMP1	EGF-containing fibulin-like ECM protein 1	201842_s_at	2.37	2.00E-06
EFEMP2	EGF-containing fibulin-like ECM protein 2	209356_x_at	1.38	7.34E-04
FBLN1	Fibulin 1	202994_s_at	1.66	7.40E-06
MGP	Matrix Gla protein	202291_s_at	3.08	$P <$ 1e-07
POSTN	Periostin, osteoblast-specific factor	210809_s_at	2.30	2.24E-03
SPP1	Secreted phosphoprotein 1 (osteopontin)	209875_s_at	3.50	2.20E-06
CILP	Cartilage intermediate layer protein	206227_at	1.76	5.00E-07
THBS2	Thrombospondin 2	203083_at	1.63	5.00E-06
THBS4	Thrombospondin 4	204776_at	2.45	6.28E-04
FBN1	Fibrillin 1	202766_s_at	2.09	1.42E-05
GPC3	Glypican 3	209220_at	1.40	9.48E-04
GPC4	Glypican 4	204983_s_at	1.64	4.92E-05
PCOLCE	ProCollagen C-endopeptidase enhancer	202465_at	2.22	$P <$ 1e-07
P4HA2	ProCollagen-proline 4-hydroxylase, alpha II	202733_at	1.66	7.10E-06
TIMP1	Tissue inhibitor of metalloproteinase 1	201666_at	3.31	$P <$ 1e-07
TIMP2*	Tissue inhibitor of metalloproteinase 2	203167_at	1.22	1.99E-05
MMP2*	Matrix metalloprotease 2	201069_at	1.41	4.76E-04
ADAM10	A disintegrin and metalloproteinase domain 10	202603_at	1.61	2.70E-06
A2M	Alpha-2-macroglobulin	217757_at	1.77	4.00E-06
LOXL2	Lysyl oxidase-like 2	202998_s_at	1.50	2.87E-04
LOXL1	Lysyl oxidase-like 1	203570_at	1.90	5.06E-05
SERPINE2	Serine (or cysteine) proteinase inhibitor 2, clade E	212190_at	1.98	9.00E-07
TGFB1	Transforming growth factor, beta 1	203085_s_at	1.65	2.90E-06
TGFB3*	Transforming growth factor, beta 3	209747_at	1.15	5.04E-03
SMAD1	SMAD, mothers against DPP homolog 1	210993_s_at	1.77	7.86E-04
TGFBI	Transforming growth factor, beta-induced, 68 kDa	201506_at	1.90	1.75E-05
TIEG	TGFB inducible early growth response	202393_s_at	0.62	5.45E-03
FSTL1	Follistatin-like 1	208782_at	2.08	1.00E-06
SERPINH1	Serine (or cysteine) proteinase inhibitor 1clade H	207714_s_at	1.64	9.08E-05

[a]Genes marked with * did not meet filtering criteria and were not listed among the 618 genes identified by the multivariate permutation test.

TABLE 2. *Genes expressed outside control range in DMD patients with high frequency*[a]

Gene symbol	Gene name	Probe set	Calls: I	Calls: D	Calls: NC
ACTC	Actin, alpha, cardiac muscle	205132_at	22	0	0
ATP1B3	ATPase, Na^+/K^+ transporting, beta 3 polypeptide	208836_at	22	0	0
C1QA	Complement component 1, q subcomponent, alpha polypeptide	218232_at	22	0	0
CSPG2	chondroitin sulfate proteoglycan 2 (versican)	204620_s_at	22	0	0
LAPTM5	Lysosomal-associated multispanning membrane protein-5	201720_s_at	22	0	0
LR8	LR8 protein	220532_s_at	22	0	0
LUM	Lumican	201744_s_at	22	0	0
LILRB1	Leukocyte immunoglobulin-like receptor, subfamily B, member 1	213975_s_at	22	0	0
MYH8	Myosin, heavy polypeptide 8, skeletal muscle, perinatal	206717_at	22	0	0
MYL4	Myosin, light polypeptide 4, alkali; atrial, embryonic	210395_x_at	22	0	0
SPP1	Secreted phosphoprotein 1, osteopontin	209875_s_at	22	0	0
TIMP1	Tissue inhibitor of metalloproteinase 1	201666_at	22	0	0
TYROBP	TYRO protein tyrosine kinase binding protein	204122_at	22	0	0
VCAM1	Vascular cell adhesion molecule 1	203868_s_at	22	0	0
ACTB	Actin, beta	200801_x_at	21	0	1
CD14	CD14 antigen	201743_at	21	0	1
CSF1R	Colony-stimulating factor 1 receptor	203104_at	21	0	1
DAB2	Disabled homolog 2, mitogen-responsive phosphoprotein	201278_at	21	0	1
FER1L3	fer-1-like 3, myoferlin	201798_s_at	21	0	1
HLA-DPA1	Major histocompatibility complex, class II, DP alpha 1	211991_s_at	21	0	1
HLA-DRA	Major histocompatibility complex, class II, DR alpha	208894_at	21	0	1
IFI16	Interferon, gamma-inducible protein 16	208966_x_at	21	0	1
ITGB2	Integrin, beta 2, antigen CD18 (p95) (mac-1) beta subunit	202803_s_at	21	0	1
LRRC17	Leucine-rich repeat containing 17	205381_at	21	0	1
LY96	Lymphocyte antigen 96	206584_at	21	0	1
MRC1	Mannose receptor, C type 1	204438_at	21	0	1
MYH3	Myosin, heavy polypeptide 3, skeletal muscle, embryonic	205940_at	21	0	1
NES	Nestin	218678_at	21	0	1
RAB31	RAB31, member RAS oncogene family	217764_s_at	21	0	1
RGS2	Regulator of G-protein signaling 2, 24 kDa	202388_at	21	0	1
TGFB1	Transforming growth factor, beta 1	203085_s_at	21	0	1
TNNT2	Troponin T2, cardiac	215389_s_at	21	0	1
TUBA6	Tubulin alpha 6	209251_x_at	21	0	1
RASA4	RAS p21 protein activator 4	208534_s_at	0	21	1
PYGM	Phosphorylase, glycogen; muscle	205577_at	0	21	1
DMD	Dystrophin	203881_s_at	0	20	2
GLUL	Glutamate-ammonia ligase	200648_s_at	0	20	2
TACC2	Transforming, acidic coiled-coil containing protein 2	211382_s_at	0	20	2
SCN1B	Sodium channel, voltage-gated, type I, beta	205508_at	0	19	3

[a]For every gene, the expression value in each of our 22 DMD patients was compared with the expression range of the same gene in our control group. I, Increased above highest value in controls; D, decreased below lower value in controls; NC, within control range.

transcripts encoding enzymes involved in glycogen metabolism, glycolysis, TCA cycle, lipid transport, and β-oxidation were down-regulated. Although the magnitude of the change was not large (0.4–0.6×), the downward modulation of this gene cluster represents a highly coordinated transcriptional change and an invariant character of this disease (3, 4) (Table 1, Muscle genes).

Dystrophin (Dp427) was decreased in 20/22 patients. Two subjects (DMD1 and DMD11) appeared to escape nonsense-mediated decay (NMD) and displayed close to normal dystrophin mRNA expression. However in both cases the protein was absent from the muscle fibers and the two children displayed typical clinical features. Moreover, they did not appear as a correlated group by cluster analysis (data not shown). A small proportion of DMD patients showing reduced dystrophin NMD have been described by Chelly *et al.* (16).

The relative abundance of most of the transcripts encoding other DGC components was normal except for syntrophin α1 (SNTA1), which was repressed, and sarcoglycan ε (SGCE), which was induced (supplemental material, DGC Components Expression).

Postnatal myogenesis relies on the activation of resident myogenic cells that proliferate throughout the regenerating muscle and differentiate to fuse into multinucleated muscle fibers (17). As cells are not synchronized and can undergo asymmetric mitosis, different phases of the myogenic program are expected to coexist in regenerating muscle.

In our patients, we observed the concomitant induction of genes involved in cell cycle progression (cyclin

G2, cyclin D2, and CDK4) and cell cycle withdrawal (CDKN1A, GAS1, and GADD45A). Genes encoding myogenic transcription factors of the bHLH and MEF family (MyoD, myogenin, and MEF2C) were also induced, indicating diffuse activation of myogenesis in DMD muscle (18).

In recent years, increasing attention has been placed on the role of the myostatin (19–21) and insulin-like growth factor 1 (IGF1) (22–25) pathways in controlling muscle trophism and myogenesis (26). In our patients, we observed increased expression of IGF1, IGF2, and IGF binding proteins 4 and 7. PRSS11, an IGFBP protease acting as negative modulator of this pathway (27), was also induced. We studied the expression of myostatin (GDF8), follistatin (FST), and follistatin-like 1 (FSTL1) by real-time rt-PCR. Both FST and FSTL1 transcripts were increased in patients whereas expression of GDF8 was often reduced, but did not reach statistical significance (**Fig. 2** and supplemental materials, Table ST2).

Three major proteolytic systems operating in muscle have been implicated in the pathophysiology of muscle atrophy and dystrophy: lysosomal proteases (CTS) (28), calpains (CAPN) (29, 30), and the ubiquitin proteasome system (31, 32). Three cathepsin genes were up-regulated (cathepsins B, C, and K), CAPN3 was repressed, and CAPN6 was induced. Genes encoding proteasome subunits were variably modulated: PSMB8 and PSME2 genes were induced and the PSMD12 repressed. Enzymes involved in protein ubiquitination (UBE2B, UBE2D1, CUL5, and FBXO3) or deubiquitination and ubiquitin recycling (USP13 and USP25) were repressed.

Inflammation

Genes involved in immune response and inflammation were massively induced in our patients, and our analysis provided a detailed description of the inflammatory response in this presymptomatic phase of the disease (Table 1, Inflammation).

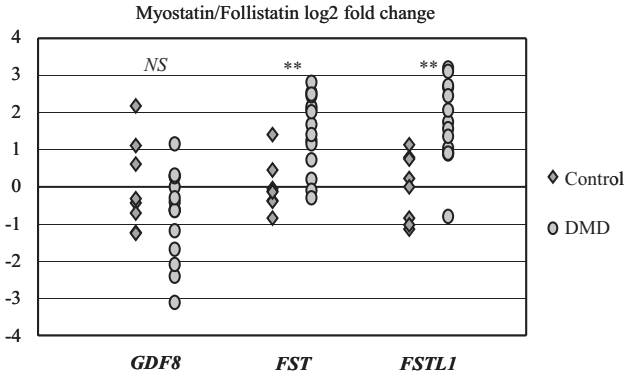

Figure 2. Real-time polymerase chain reaction (PCR) analysis of myostatin (GDF8), follistatin (FST), and follistatin-like 1 (FSTL1) gene expression. DMD muscle displays a consistent alteration in the pattern of expression of genes involved in myostatin signaling. Changes in transcript abundance are expressed as log2 ratio to control mean. Significance was assessed by *t* test; $^{**}P < 0.01$; NS, not significant.

We observed increased expression of class I and II MHC, components of the complement system (C1, C3, and the H factor), a set of IFN-inducible genes, and markers of infiltrating immune cells. Four chemokines (CCL14, CCL2, CXCL12, and CXCL14) were also induced. Among these, CXCL14 has been shown recently to be a potent chemoattractant and activator of dendritic cells (DC) and is suggested to be involved in DC homing (33). A robust inflammatory response was recently reported in four patients aged 8–10 months and ascribed to early activation of the NF-κB pathway by TLR7 (34). Accordingly, both TLR7 and class I MHC and VIM reported by the authors as NF-κB target genes were induced in our patients since early postnatal life. In line with the idea that exaggerated NF-κB activation may exert a detrimental effect over the course of the disease, pharmacological inhibition of this pathway was reported to ameliorate the *mdx* pathology (35, 36).

Fibrosis

The steady-state amount and composition of the ECM that surrounds cells in solid tissues rely on a balance between deposition of structural components and remodeling (37).

Our patients showed increased expression of a large number of genes encoding ECM components and enzymes involved in matrix biosynthesis and remodeling (Table 1, ECM remodeling). Type I and III collagen, lumican, and asporin showed the largest fold changes whereas other collagen types (type IV, V, VI, XIV, XV, and XVIII), fibronectin, laminins, elastin, and proteoglycans (chondroitin sulfate, heparan sulfate, and small leucine-rich type) were induced to a lesser extent. In this framework, we found increased expression of the matrix metalloproteinase MMP2 and two MMPs inhibitors: TIMP1 and TIMP2. Von Moers *et al.* (38), by describing a similar expression pattern in DMD patients aged 3.5–15 years suggested that an unbalance in MMP1/TIMP1 stoichiometry characterizes DMD muscle and contributes to progressive fibrosis. Since these alterations were already present in our 1.5-month-old patient, increased ECM synthesis and inhibition of fibrolytic activity are early events in DMD. TIMP1 expression can be induced in response to cytokines and hormones and has been linked to the development of pulmonary and liver fibrosis (39, 40). Among such cytokines, the TGF-β family of multifunctional cytokines controls proliferation, differentiation, and other cellular activities by acting as negative autocrine growth factors (41). Three members of the TGF-β family (namely, TGFB1, TGFB2, and TGFB3) are known to participate in tissue regeneration. Deregulation in their signaling is implicated in the development of organ fibrosis and scar formation. The increased expression of these cytokines has been described in DMD patients and in *mdx* mice (38, 42–46).

In our young patients, TGFB1 was the predominant

TGF-β isoform induced, being expressed above all controls in all patients but one (Table 2, **Fig. 3**). In agreement with earlier studies reporting its overexpression in advanced DMD (3, 4, 34), TGFB3 was expressed above control mean in 18 of 22 patients. However, TGFB3 was induced to a lesser extent than TGFB1, and only in patients older than 6 months (Fig. 3).

Decorin (DCN) and dermatopontin are known modulators of TGF-β activity and were both induced. These proteins can individually elicit opposite regulatory effects on TGF-β signaling but, when coexpressed, form a stable complex, with inhibitory activity (47). A recent report described the reduced expression of DCN mRNA in DMD patients aged 2–8 years (48). In our data set, four independent probesets showed superimposable results ($0.93<R^2<0.95$, among three probesets), indicating increased DCN expression.

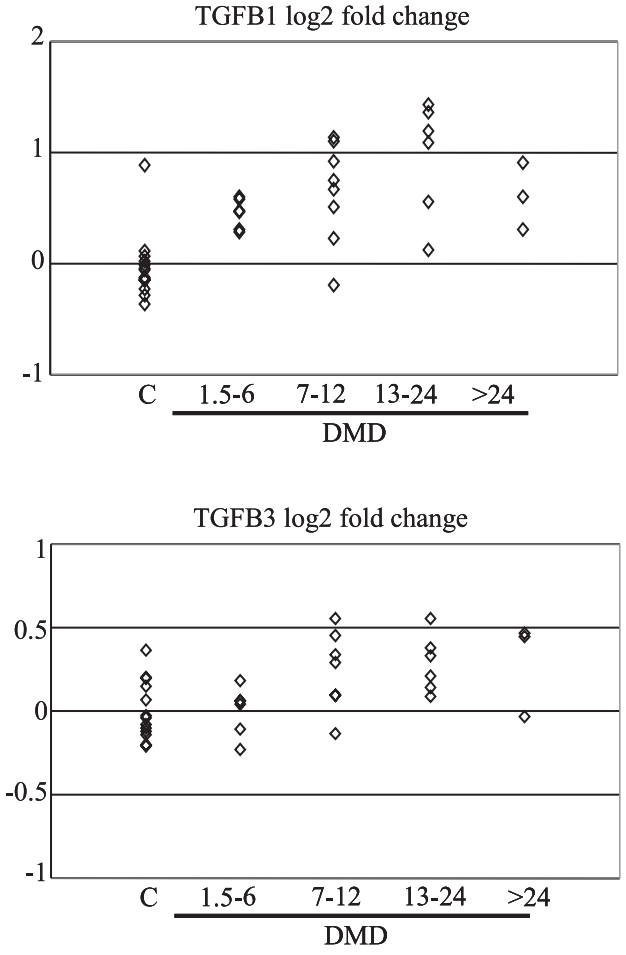

Figure 3. Expression of TGFβ cytokines in DMD muscle as a function of patient age. TGFB1 and TGFB3 are induced at different times in the progression of the disease. TGFB1 was the predominant TGF-β isoform overexpressed in our patients, being induced as early as at 1.5 months of age. TGFB3 was expressed above control mean in 18/22 patients, but was induced to a lesser extent than TGFB1 and only in patients older than 6 months. Changes in transcript abundance are expressed as log2 ratio to control mean.

DMD progression does not represent a major factor affecting muscle tissue expression profile

An original goal of this study was to identify gene expression alterations in the skeletal muscle of presymptomatic DMD children, which may represent molecular landmarks for progression of the disease. In our cohort of infant patients (19/22 aged 1.5 to 22 months), clustering analysis did not display patient groupings by age, showing that age is not a major variable affecting gene expression in DMD muscle.

Since function-related gene clusters rather than single genes may represent and describe the progression of the DMD more comprehensively, we generated four lists of transcripts representative of four key aspects of disease pathophysiology: muscle regeneration, inflammation, ECM remodeling, and energy metabolism (supplemental materials, Genelist_Pathogenic Components). Following the expression trends of these clusters in the natural history of the disease, we show that, from a transcriptional point of view, three of these components are already fully activated in the younger patients studied. The muscle regeneration cluster only is progressively induced during the first months of postnatal life (**Fig. 4**).

We also compared our results with those reported in earlier studies based on the Affymetrix technology.

Besides the overall good agreement on transcripts and pathways modulated in DMD that has already been mentioned, all genes that were considered relevant and singularly discussed by other authors (3–7) were confirmed in our patients. Remarkably, we were able to compare at the single gene level our results with those reported by Haslet *et al.* (4), whose study design was similar to ours (supplemental material, Table ST3): of the 105 genes scored by the authors as differentially expressed ($P<$1E-4 and mean fold change>2), 87 (83%) turned out to be differentially expressed within the same probability threshold in our data set, 95 (90%) within $P<$ 1E-3, and 104 (99%) within $P<$ 5E-2 whereas only one showed a probability higher than 0.05 (FADS3, 0.0538). The comparison showed that all of the genes reported by the authors as modulated in advanced DMD with high confidence were similarly modulated in our presymptomatic patients. This result also suggests that cross-experiment analysis of the distribution of *P* values within differentially expressed gene lists measures and describes the level of congruence between independent experiments better than the widely used degree of overlap between the same lists.

Correlation analysis identifies genes induced or repressed with patient age

Longitudinal analysis of time-series microarray data has been used to describe dynamic expression changes occurring in the progression of the *mdx* pathology as well as the response to specific acute events like experimentally induced muscle damage or denervation. As

unsupervised clustering would not highlight the effect of the covariate "age" if it affected the expression of a small number of genes, we analyzed our patients as a time series searching for genes that are induced or repressed along the natural history of the disease. We made use of correlation analysis to search for genes modulated across 4 age-defined classes of patients: 1.5–6, 7–12, 13–24, and 25–60 months. Using this approach, we identified a small number of genes whose expression is either increased or decreased in patients but not in controls as a function of age (supplemental material, DMDAGECORR).

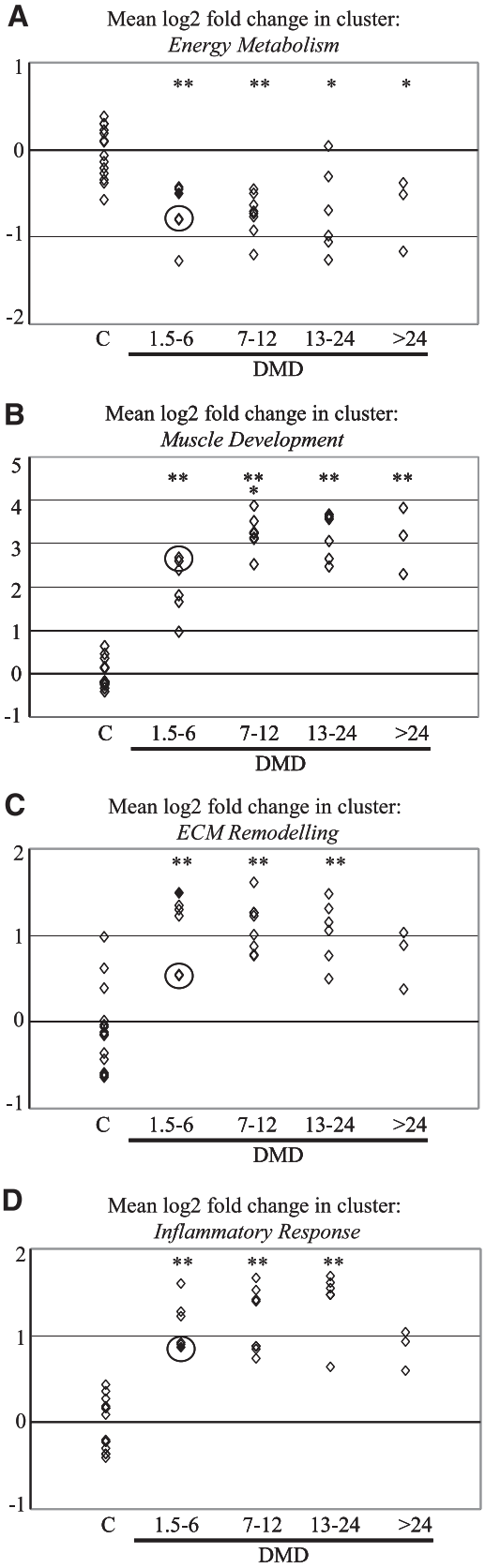

Figure 4. Pathogenic components analysis. To represent the extent of activation of four major pathophysiological aspects of the DMD along the progression of the disease, we computed the average fold change of four clusters of differentially expressed genes involved in relevant biological processes, showing correlated expression trends across the data set by gene clustering (Supplemental Materials, Genelist_Pathogenic Components). The timing of induction of these components was visualized by plotting this index as a function of patient age at biopsy. We also plotted in the graph the value for the DMD3_rep sample, a technical replicate of the DMD3 sample (*de novo* labeling of the same RNA and hybridization in an independent experimental session). The DMD3 and the DMD3_rep measures (shown within the circle) were always superimposed in the graph, underscoring the reproducibility of the analysis. Changes are expressed as log2 ratio to control mean. Significance was assessed by *t* test; $*P < 0.05$, $**P < 0.01$. For the muscle development cluster only (*B*), the significance of the *t* test is also reported for the 1.5–6 month *vs.* 7–12 month comparison.

Table 3 reports 16 genes correlated to patients' ages with *P* values lower than 5E-04. Among these, GPSM2, encoding a cytoplasmic regulator of G-protein signaling involved in mitotic spindle movements and cell cycle progression, showed the highest *P* value and correlation coefficient (**Fig. 5*A***). The increased expression of this gene with patient age was further confirmed by a second probe set interrogating the same transcript. Other genes similarly induced include FRZB1, also independently scored by two probe sets, and OXCT1, a key metabolic enzyme that catalyzes a rate-limiting step in the metabolism of ketone bodies (Fig. 5*B, C*). The higher expression of this gene in older patients is consistent with the elevation of plasma ketone bodies reported in advanced DMD (49, 50). FRZB1 is a member of the soluble frizzled related proteins family (SFRPs) of Wnt inhibitors. Activation of Wnt signaling is required to sustain proliferation of vessel-derived mesenchimal progenitors (mesoangioblasts) and is also able to induce myogenic specification of muscle-derived $SCA1^+$ SP cells and circulating $AC133^+$ cells (51–54). FRZB1 and other sFRP members have been shown to antagonize Wnt signaling in these cell types. SFRP4, another member of the inhibitory SFRP family, was similarly induced with patient age.

Among genes progressively down-regulated, COL4A1, POSTN, and DLK1 (Fig. 5*D–F*) showed the highest *P* values followed by ADAMTSL3 and GREM2. It should be noted that although the expression of these genes decreases with patient age, they are not underexpressed in patients. These three genes are highly induced in early postnatal DMD muscle but, after a decreasing trend, their expression is normalized by the end of the second year.

TABLE 3. *Top-scoring genes from correlation analysis*[a]

Gene symbol	Description	Probe set	Correlation	*P* value	Age dependence in controls
GPSM2	G-protein signaling modulator 2	221922_at	0.828	1.90E-06	NO
GPSM2	G-protein signaling modulator 2	205240_at	0.734	1.03E-04	NO
ITIH4	Inter-alpha inhibitor H4	206287_s_at	0.766	3.18E-05	NO
OXCT1	3-oxoacid CoA transferase 1	202780_at	0.755	4.89E-05	NO
DDN	Dendrin	214788_x_at	0.729	1.25E-04	NO
MAPRE3	Microtubule-associated protein, RP/EB 3	203841_x_at	0.696	3.21E-04	YES
C6orf106	Chromosome 6 open reading frame 106	217924_at	0.685	4.42E-05	YES
FRZB	Frizzled-related protein	203698_s_at	0.682	4.78E-04	NO
FRZB	Frizzled-related protein	203697_at	0.667	6.94E-04	NO
BGN	Biglycan	201262_s_at	0.679	5.10E-04	NO
PRCP	Prolylcarboxypeptidase (angiotensinase C)	201494_at	−0.699	2.96E-04	NO
IMP-2	IGF-II mRNA binding protein 2	218847_at	−0.699	3.04E-04	NO
RBM8A	RNA binding motif protein 8A	213852_at	−0.713	2.04E-04	NO
GREM2	Gremlin 2 homolog	220794_at	−0.718	1.70E-04	NO
ADAMTSL3	ADAMTS-like 3	213974_at	−0.769	2.81E-05	NO
DLK1	Delta-like 1 homolog	209560_s_at	−0.776	2.08E-05	NO
POSTN	Periostin	210809_s_at	−0.794	8.60E-06	YES
COL4A1	Collagen, type IV, alpha 1	211980_at	−0.812	3.50E-06	NO

[a]Genes whose expression was either increased or decreased in patients as a function of age were identified by correlation analysis across four classes of patients: 1.5–6, 7–12, 13–24, and 25–60 months. Age dependence in controls was assessed as described in Materials and Methods.

DLK1, also known as preadipocyte factor 1 (PREF1), is a human homologue of the *Drosophila* Notch ligand delta. The product of this gene represses adipogenic differentiation in a variety of experimental models (55, 56) and can also affect muscle trophism. In *callipyge* sheep, the increased expression of DLK1 has been causally associated with the muscular phenotype and hypertrophy of type II fibers that characterize these animals (57).

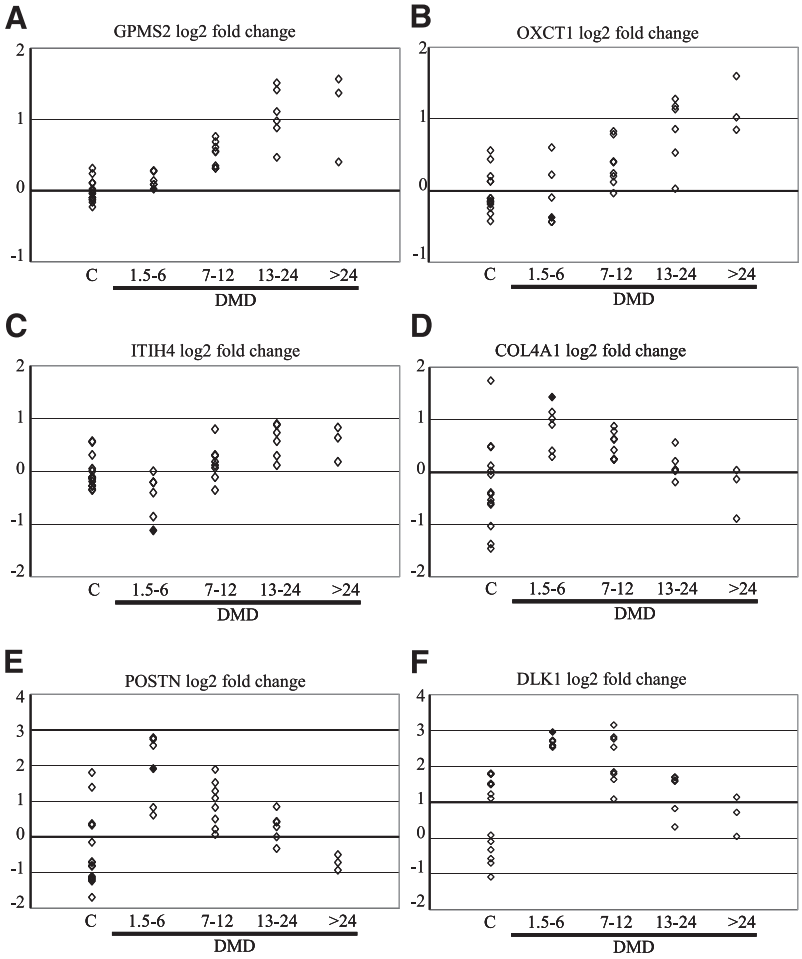

Figure 5. Selected genes from correlation analysis. Genes whose expression increases or decreases with patient age were identified by correlation analysis. Changes in transcript abundance are expressed as log2 ratio to control mean.

GREM2 is a member of the Cerberus and Dan family of BMP antagonists that play a role in regulating organogenesis, body patterning, and tissue differentiation (58, 59). BMP signaling promotes osteoblastic specification in different types of potentially myogenic cells like the C2C12 cell line, mesoangioblasts, and other populations of muscle-derived stem cells (54, 60, 61). Taken together, the results of our correlation analysis show that expression of individual genes changes as a function of patient age.

Real-time rt-PCR

We validated by real-time PCR some of the gene expression changes identified by microarray analysis as well as a number of genes we considered relevant to the disease (CHRNE, CHRNG, GDF8, FST, and FSTL1). All of the genes further analyzed showed expression changes consistent with those estimated by gene chip analysis (supplemental material, Table ST2). In general, PCR-based expression change estimates were larger than those observed in the microarray study.

DISCUSSION

In recent years, gene chip analysis has been successfully used to capture a high-resolution snapshot of the altered transcriptional state that characterizes dystrophin-deficient muscle in humans and in animal models (3–7, 34, 62–66). By studying the expression profile of 19 DMD patients younger than 2 years, we have described with high resolution the gene expression signature that characterizes DMD muscle during the initial or presymptomatic phase of the disease. As a result, we show that, in the first 2 years, DMD muscle is already set to express a distinctive gene expression pattern considerably different from the one expressed by normal, age-matched muscle. This dystrophic signature is characterized by the altered expression of genes involved in the inflammatory response, ECM remodeling, muscle regeneration, and energy metabolism and appears to be conserved across the analyzed age range. Accordingly, cluster analysis did not group patients by age and was unable to sort the younger, presymptomatic patients ($n=6$, age<6 months) from the two symptomatic ones (age 4 and 5 years). Consistent with the idea that disease progression does not introduce major changes in muscle expression profile, the gene expression signature that characterizes our patients faithfully reproduces the alterations described in later stages of the disease (3–7). Since our youngest patient was 1.5 months of age, this alteration is congenital or develops perinatally, being maintained throughout the course of the disease.

However, as pathological findings can be observed in muscle sections of presymptomatic patients, it is not surprising that our infant patients shared a dystrophic signature with the older ones. Nevertheless, many of the observations reported in our study had not been described in human patients, and the information provided by our analysis complements and integrates the great amount of transcriptional data available on more advanced DMD muscle.

Notably, the timing of induction of the molecular pathology in DMD appears different from the one described in *mdx* mice, in which minimal transcriptional alterations were shown to characterize the initial prenecrotic phase of the disease, whereas later phases were contrasted by parallel changes in transcriptome composition (62–64).

Our attention was drawn to three elements of this complex picture because of their potential relevance to the clinical progression of the disease and to the development of therapeutic strategies: *1)* extensive induction of inflammation; *2)* the presence of a fibrogenic signature; *3)* progressive establishment of an unfavorable pattern of morphogenetic signaling.

In a recent study addressing the issue of the evolution of muscle expression profile in the natural history of the DMD, Chen *et al.* showed that a chronic inflammatory response characterizes presymptomatic DMD muscle (34). Although the general traits of the transcriptional alterations in this preclinical phase of the disease are poorly described, many of the observations reported by the authors hold true in our data set. As highlighted by the large number of genes involved in immune function induced in our young patients, our study provides a robust statistical foundation for their findings and extends the observation to patients as young as 1.5 months. It is worth noting that the inflammatory component identified in our patients is larger than previously estimated, questioning the idea that inflammation is induced to a lesser extent in DMD than in *mdx* pathology. Accordingly, ~67% of the inflammatory genes reported as induced in *mdx* mice (64) displayed similar behavior in our patients.

We show that other aspects of the molecular pathology of the disease are also induced early in the natural history of DMD. Among these, a fibrogenic signature consisting of a large number of genes whose products participate to the protein makeup of fibrotic formations or function in ECM remodeling is prominent in our patients, even though only negligible signs of fibrosis can be observed at this stage of the disease. This signature does not appear sufficient *per se* to induce progressive ECM accumulation and fibrosis. A similar pattern of gene expression can be observed in immunomediated muscle inflammatory diseases (refs. 65, 66 and our unpublished data) where, upon timely pharmacological intervention, muscle regeneration can occur efficiently, and abnormal matrix deposition and scar formation can be prevented. This is also consistent with the observation that, in *mdx* mice, a common fibrogenic signature is shared by the diaphragm and the quadriceps muscles, although only the former undergoes progressive fibrosis (46, 62, 63).

Infiltration of muscle by phagocytic inflammatory cells and induction of ECM synthesis and remodeling are commonly observed during muscle regeneration

(67–69), and a large part of the transcriptional alterations described may therefore reflect the permanent regenerative state to which DMD muscle is set. Muscle regeneration does not necessarily result in abnormal matrix deposition and scar formation, but in several instances represents an effective means to ensure tissue plasticity and replace damaged fibers. Concurrent mechanisms, involving a persistent imbalance between ECM synthesis and degradation and a decrease in muscle regenerative capacity, contribute to determining the inability of DMD muscle to complete an effective regenerative process. Although progressive depletion of the satellite cells compartment is still a leading hypothesis to explain the inability of DMD muscle to support lifelong the high turnover rate demanded by recurrent myofiber injury, current evidence suggests that tissue microenvironmental factors may contribute to the progressive loss of regenerative capacity that characterizes the advanced stages of the disease (70, 71). In a recent work, Conboy *et al.* showed that age-dependent attenuation of Notch signaling is the cause of the decreased ability of aged muscle to regenerate (72, 73). Exogenous stimulation of this pathway was able to rejuvenate satellite cells and restore regenerative potential to old muscles (72, 73), supporting the notion that muscle regeneration may be pharmacologically controlled. This may also suggest that abnormalities in muscle regeneration may arise from postnatal defects in morphogenetic signaling.

Four genes identified by our correlation analysis encode extracellular or membrane-bound proteins functioning in ligand/receptor interactions upstream of one of the Wnt, Notch, and BMP pathways. Changes in the activation state of each of these pathways may influence cell cycle progression and fate decisions in some potentially myogenic, mesenchimal stem cell populations (51–61). We may speculate that the altered expression of these signaling molecules offers evidence of the establishment of a nonpermissive tissue microenvironment and that abnormal morphogenetic signaling may interfere with the regenerative capacity of DMD muscle by preventing proliferation of myogenic progenitors and/or their commitment to a myogenic fate.

We consider the correlation across patient age a significant aspect of our analysis, as it provides evidence that the expression of genes changes along the natural history of DMD. It is conceivable that applying a similar approach to a large number of patients whose ages scatter over a range representative of the full evolution of the disease may highlight aspects of DMD pathophysiology that, because of their evolutive nature, have so far escaped the common patients *vs.* controls experimental design.

In conclusion, the demonstration that most of the molecular aspects contributing to the pathophysiology of DMD are already induced in infant patients, in agreement with previous evidence supported by histological and immunohistochemical findings, supports the idea of precocious therapeutic interventions for the disease (34). Furthermore, as microarray analysis has been proposed as a tool to evaluate the effects of therapy in DMD and *mdx* mice (74–76), our study, by providing the basic reference knowledge required, laid the ground for application of this technology to evaluate the effects of therapy in preclinical DMD children.

SUPPLEMENTAL MATERIAL

Supplemental Tables ST1, ST2, and ST3 and files MIAME Compliance, DMDDATA_rma, GeneChip QC, DMDCLASSCOMP, DMDGO, DMDAGECORR, Genelist_Pathogenic Components, DGC_Components Expression, and Supplemental Information_Materials and Methods are available at www.fasebj.org. The 37 microarray data set is available at http://www.ncbi.nlm.nih.gov/geo/ and under accession #GSE6011. FJ

Microarray experiments were conducted in the Catholic University Microarray Core Laboratory. We are grateful to Andrea Brancaccio (Catholic University, Rome) and Mauro Helmer-Citterich, Stefano Volinia, and Diego Arcelli (DAMA Telethon Facility, Modena) for helpful hints and discussions. This work was funded by MIUR (2004) and the "Ministero Italiano della Salute." Thanks are due to "Parent Project Italia" for their generous support.

REFERENCES

1. Hoffman, E. P., Brown, R. H., Jr., and Kunkel, L. M. (1987) Dystrophin: the protein product of the Duchenne muscular dystrophy locus. *Cell* **51,** 919–928
2. Straub, V., and Campbell, K. P. (1997) Muscular Dystrophies and the dystrophin-glycoprotein complex. *Curr. Opin. Neurol.* **10,** 168–175 (review)
3. Chen, Y-W., Zhao, P., Borup, R., and Hoffman, E. P. (2000) Expression profiling in the muscular dystrophies: identification of novel aspects of molecular pathophysiology. *J. Cell Biol.* **151,** 1321–1336
4. Haslett, J. N., Sanoudou, D., Kho, A. T., Bennett, R. R., Greenberg, S., Kohane, I. S., Beggs, A. H., and Kunkel, L. M. (2002) Gene expression comparison of biopsies from Duchenne muscular dystrophy (DMD) and normal skeletal muscle. *Proc. Natl. Acad. Sci. U. S. A.* **99,** 15000–15005
5. Bakay, M., Zhao, P., Chen, J., and Hoffman, E. P. (2002) A web-accessible complete transcriptome of normal human and DMD muscle. *Neuromuscul. Disord. Suppl.* **1,** S125–S141
6. Bakay, M., Chen, Y. W., Borup, R., Zhao, P., Nagaraju, K., and Hoffman, E. P. (2002) Sources of variability and effect of experimental approach on expression profiling data interpretation. *BMC Bioinformatics* **3,** 4
7. Haslett, J. N., Sanoudou, D., Kho, A. T., Han, M., Bennett, R. R., Kohane, I. S., Beggs, A., and Kunkel, L. M. (2003) Gene expression profiling of Duchenne muscular dystrophy skeletal muscle. *Neurogenetics* **4,** 163–171
8. Simon, R., Korn, E., McShane, L., Radmacher, M., Wright, G., and Zhao, Y. (2003) *Design and Analysis of DNA Microarray Investigations,* Springer-Verlag, New York
9. Korn, E. L., Troenndle, J. F., McShane, L. M., and Simon, R. (2003) Controlling the number of false discoveries: Application to high-dimensional genomic data. *J. Stat. Plan. Inference* **124,** 2448–2455
10. Simon, R., and Lam, A. *BRB-ArrayTools User Guide, version 3.2.* Biometric Research Branch, National Cancer Institute, NIH. http://linus.nci.nih.gov/brb

11. Irizarry, R. A., Bolstad, B. M., Collin, F., Cope, L. M., Hobbs, B., and Speed, T. P. (2003) Summaries of Affymetrix GeneChip probe level data. *Nucleic Acids Res.* **31,** e15
12. Pavlidis, P., Weston, J., Cai, J., and Noble, W. S. (2002) Learning gene functional classifications from multiple data types. *J. Comput. Biol.* **9,** 401–411
13. Pizon, V., Gerbal, F., Diaz, C. C., and Karsenti, E. (2005) Microtubule-dependent transport and organization of sarcomeric myosin during skeletal muscle differentiation. *EMBO J.* **24,** 3781–3792
14. Mishina, M., Takai, T., Imoto, K., Noda, M., Takahashi, T., Numa, S., Methfessel, C., and Sakmann, B. (1986) Molecular distinction between fetal and adult forms of muscle acetylcholine receptor. *Nature* **321,** 406–411
15. Gu, Y., and Hall, Z. W. (1988) Immunological evidence for a change in subunits of the acetylcholine receptor in developing and denervated rat muscle. *Neuron* **1,** 117–125
16. Chelly, J., Gilgenkrantz, H., Lambert, M., Hamard, G., Chafey, P., Recan, D., Katz, P., de la Chapelle, A., Koenig, M., Ginjaar, I. B., *et al.* (1990) Effect of dystrophin gene deletions on mRNA levels and processing in Duchenne and Becker muscular dystrophies. *Cell* **63,** 1239–1248
17. Grounds, M. D. (1991) Towards understanding skeletal muscle regeneration. *Pathol. Res. Pract.* **187,** 1–22
18. Weintraub, H. (1993) The MyoD family and myogenesis: redundancy, networks, and thresholds. *Cell* **75,** 1241–1244
19. Lee, S. J. (2004) Regulation of muscle mass by myostatin. *Annu. Rev. Cell Dev. Biol.* **20,** 61–86
20. Schuelke, M., Wagner, K. R., Stolz, L. E., Hubner, C., Riebel, T., Komen, W., Braun, T., Tobin, J. F., and Lee, S. J. (2004) Myostatin mutation associated with gross muscle hypertrophy in a child. *N. Engl. J. Med.* **350,** 2682–2688
21. Jackman, R. W., and Kandarian, S. C. (2004) The molecular basis of skeletal muscle atrophy. *Am. J. Physiol.* **287,** C834–C843
22. Winn, N., Paul, A., Musaro, A., and Rosenthal, N. (2002) Insulin-like growth factor isoforms in skeletal muscle aging, regeneration, and disease. *Cold Spring Harb. Symp. Quant. Biol.* **67,** 507–518
23. Broccolini, A., Ricci, E., Pescatori, M., Papacci, M., Gliubizzi, C., D'Amico, A., Servidei, S., Tonali, P., and Mirabella, M. (2004) Insulin-like growth factor I in inclusion-body myositis and human muscle cultures. *J. Neuropathol. Exp. Neurol.* **63,** 650–659
24. Musaro, A., Giacinti, C., Borsellino, G., Dobrowolny, G., Pelosi, L., Cairns, L., Ottolenghi, S., Cossu, G., Bernardi, G., Battistini, L., *et al.* (2004) Stem cell-mediated muscle regeneration is enhanced by local isoform of insulin-like growth factor 1. *Proc. Natl. Acad. Sci. U. S. A.* **101,** 1206–1210
25. Barton, E. R., Morris, L., Musaro, A., Rosenthal, N., and Sweeney, H. L. (2002) Muscle-specific expression of insulin-like growth factor I counters muscle decline in mdx mice. *J. Cell Biol.* **157,** 137–148
26. Engvall, E., and Wewer, U. M. (2003) The new frontier in muscular dystrophy research: booster genes. *FASEB J.* **17,** 1579–1584
27. Zumbrunn, J., and Trueb, B. (1996) Primary structure of a putative serine protease specific for IGF-binding proteins. *FEBS Lett.* **398,** 187–192
28. Kominami, E., Kunio, I., and Katunuma, N. (1987) Activation of the intramyofibral autophagic-lysosomal system in muscular dystrophy. *Am. J. Pathol.* **127,** 461–466
29. Spencer, M. J., and Mellgren, R. L. (2002) Overexpression of a calpastatin transgene in mdx muscle reduces dystrophic pathology. *Hum. Mol. Genet.* **11,** 2645–2655
30. Tidball, J. G., and Spencer, M. J. (2000) Calpains and muscular dystrophies. *Int. J. Biochem. Cell Biol.* **32,** 1–5
31. Combaret, L., Taillandier, D., Voisin, L., Samuels, S. E., Boespflug-Tanguy, O., and Attaix, D. (1996) No alteration in gene expression of components of the ubiquitin-proteasome proteolytic pathway in dystrophin-deficient muscles. *FEBS Lett.* **393,** 292–296
32. Bonuccelli, G., Sotgia, F., Schubert, W., Park, D. S., Frank, P. G., Woodman, S. E., Insabato, L., Cammer, M., Minetti, C., and Lisanti, M. P. (2003) Proteasome inhibitor (MG-132) treatment of mdx mice rescues the expression and membrane localization of dystrophin and dystrophin-associated proteins. *Am. J. Pathol.* **163,** 1663–1675
33. Shurin, G. V., Ferris, R. L., Tourkova, I. L., Perez, L., Lokshin, A., Balkir, L., Collins, B., Chatta, G. S., and Shurin, M. R. (2005) Loss of new chemokine CXCL14 in tumor tissue is associated with low infiltration by dendritic cells (DC), while restoration of human CXCL14 expression in tumor cells causes attraction of DC both in vitro and in vivo. *J. Immunol.* **174,** 5490–5498
34. Chen, Y. W., Nagaraju, K., Bakay, M., McIntyre, O., Rawat, R., Shi, R., and Hoffman, E. P. (2005) Early onset of inflammation and later involvement of TGFbeta in Duchenne muscular dystrophy. *Neurology* **65,** 826–834
35. Messina, S., Bitto, A., Aguennouz, M., Minutoli, L., Monici, M. C., Altavilla, D., Squadrito, F., and Vita, G. (2006) Nuclear factor kappa-B blockade reduces skeletal muscle degeneration and enhances muscle function in Mdx mice. *Exp. Neurol.* **198,** 234–241
36. Messina, S., Altavilla, D., Aguennouz, M., Seminara, P., Minutoli, L., Monici, M. C., Bitto, A., Mazzeo, A., Marini, H., Squadrito, F., and Vita, G. (2006) Lipid peroxidation inhibition blunts nuclear factor-kappaB activation, reduces skeletal muscle degeneration, and enhances muscle function in mdx mice. *Am. J. Pathol.* **168,** 918–926
37. Stamenkovic, I. (2003) Extracellular matrix remodelling: the role of matrix metalloproteinases. *J. Pathol.* **200,** 448–464 (review)
38. Von Moers, A., Zwirner, A., Reinhold, A., Bruckmann, O., van Landeghem, F., Stoltenburg-Didinger, G., Schuppan, D., Herbst, H., and Schuelke, M. (2005) Increased mRNA expression of tissue inhibitors of metalloproteinase-1 and -2 in Duchenne muscular dystrophy. *Acta Neuropathol. (Berlin)* **109,** 285–293
39. Arthur, M. J., Iredale, J. P., and Mann, D. A. (1999) Tissue inhibitors of metalloproteinases: role in liver fibrosis and alcoholic liver disease. *Alcohol. Clin. Exp. Res.* **23,** 940–943 (review)
40. Gueders, M. M., Foidart, J. M., Noel, A., and Cataldo, D. D. (2006) Matrix metalloproteinases (MMPs) and tissue inhibitors of MMPs in the respiratory tract: potential implications in asthma and other lung diseases. *Eur. J. Pharmacol.* **533,** 133–144 (review)
41. Leask, A., and Abraham, D. J. (2004) TGF-beta signalling and the fibrotic response. *FASEB J.* **18,** 816–827 (review)
42. Yamazaki, M., Minota, S., Sakurai, H., Miyazono, K., Yamada, A., Kanazawa, I., and Kawai, M. (1994) Expression of transforming growth factor-beta 1 and its relation to endomysial fibrosis in progressive muscular dystrophy. *Am. J. Pathol.* **144,** 221–226
43. Lundberg, I., Brengman, J. M., and Engel, A. G. (1995) Analysis of cytokine expression in muscle in inflammatory myopathies, Duchenne dystrophy, and non-weak controls. *J. Neuroimmunol.* **63,** 9–16
44. Bernasconi, P., Torchiana, E., Confalonieri, P., Brugnoni, R., Barresi, R., Mora, M., Cornelio, F., Morandi, L., and Mantegazza, R. (1995) Expression of transforming growth factor-beta 1 in dystrophic patient muscles correlates with fibrosis. Pathogenetic role of a fibrogenic cytokine. *J. Clin. Invest.* **96,** 1137–1144
45. Gosselin, L. E., Williams, J. E., Deering, M., Brazeau, D., Koury, S., and Martinez, D. A. (2004) Localization and early time course of TGF-beta 1 mRNA expression in dystrophic muscle. *Muscle Nerve* **30,** 645–653
46. Zhou, L., Porter, J. D., Cheng, G., Gong, B., Hatala, D. A., Merriam, A. P., Zhou, X., Rafael, J. A., and Kaminski, H. J. (2006) Temporal and spatial mRNA expression patterns of TGF-beta1, 2, 3 and TbetaRI, II, III in skeletal muscles of mdx mice. *Neuromuscul. Disord.* **16,** 32–38
47. Okamoto, O., Fujiwara, S., Abe, M., and Sato, Y. (1999) Dermatopontin interacts with transforming growth factor beta and enhances its biological activity. *Biochem. J.* **337,** 537–541
48. Zanotti, S., Negri, T., Cappelletti, C., Bernasconi, P., Canioni, E., Di Blasi, C., Pegoraro, E., Angelini, C., Ciscato, P., Prelle, A., Mantegazza, R., *et al.* (2005) Decorin and biglycan expression is differentially altered in several muscular dystrophies. *Brain* **128,** 2546–2555
49. Nishio, H., Wada, H., Matsuo, T., Horikawa, H., Takahashi, K., Nakajima, T, Matsuo, M., and Nakamura, H. (1990) Glucose, free fatty acid and ketone body metabolism in Duchenne muscular dystrophy. *Brain Dev.* **12**, 390–402
50. Honke, K., Hasui, M., and Takano, N. (1997) Abnormal metabolism of fatty acids and ketone bodies in Duchenne muscular

dystrophy, and the effect of biotin on these abnormalities *No To Hattatsu* **29,** 13–18 (Japanese)
51. Polesskaya, A., Seale, P., and Rudnicki, M. A. (2003) Wnt signalling induces the myogenic specification of resident CD45+ adult stem cells during muscle regeneration. *Cell* **113,** 841–852
52. Seale, P., Polesskaya, A., and Rudnicki, M. A. (2003) Adult stem cell specification by Wnt signalling in muscle regeneration. *Cell Cycle* **2,** 418–419 (review)
53. Torrente, Y., Belicchi, M., Sampaolesi, M., Pisati, F., Meregalli, M., D'Antona, G., Tonlorenzi, R., Porretti, L., Gavina, M., Mamchaoui, K., *et al.* (2004) Human circulating AC133(+) stem cells restore dystrophin expression and ameliorate function in dystrophic skeletal muscle. *J. Clin. Invest.* **114,** 182–195
54. Tagliafico, E., Brunelli, S., Bergamaschi, A., De Angelis, L., Scardigli, R., Galli, D., Battini, R., Bianco, P., Ferrari, S., Cossu, G., and Ferrari, S. (2004) TGFbeta/BMP activate the smooth muscle/bone differentiation programs in mesoangioblasts. *J. Cell Sci.* **117,** 4377–4388
55. Garces, C., Ruiz-Hidalgo, M. J., Bonvini, E., Goldstein, J., and Laborda, J. (1999) Adipocyte differentiation is modulated by secreted delta-like (dlk) variants and requires the expression of membrane-associated dlk. *Differentiation* **64,** 103–114
56. Smas, C. M., Chen, L., and Sul, H. S. (1997) Cleavage of membrane-associated pref-1 generates a soluble inhibitor of adipocyte differentiation. *Mol. Cell. Biol.* **17,** 977–988
57. Davis, E., Jensen, C. H., Schroder, H. D., Farnir, F., Shay-Hadfield, T., Kliem, A., Cockett, N., Georges, M., and Charlier, C. (2004) Ectopic expression of DLK1 protein in skeletal muscle of padumnal heterozygotes causes the callipyge phenotype. *Curr. Biol.* **14,** 1858–1862
58. Balemans, W., and Van Hul, W. (2002) Extracellular regulation of BMP signalling in vertebrates: a cocktail of modulators. *Dev. Biol.* **250,** 231–250 (review)
59. Katoh, M., and Katoh, M. (2006) CER1 is a common target of WNT and NODAL signalling pathways in human embryonic stem cells. *Int. J. Mol. Med.* **17,** 795–799
60. Musgrave, D. S., Pruchnic, R., Wright, V., Bosch, P., Ghivizzani, S. C., Robbins, P. D., and Huard, J. (2001) The effect of bone morphogenetic protein-2 expression on the early fate of skeletal muscle-derived cells. *Bone* **28,** 499–506
61. Dahlqvist, C., Blokzijl, A., Chapman, G., Falk, A., Dannaeus, K., Ibanez, C. F., and Lendahl, U. (2003) Functional Notch signalling is required for BMP4-induced inhibition of myogenic differentiation. *Development* **130,** 6089–6099
62. Porter, J. D., Merriam, A. P., Leahy, P., Gong, B., and Khanna, S. (2003) Dissection of temporal gene expression signatures of affected and spared muscle groups in dystrophin-deficient (mdx) mice. *Hum. Mol. Genet.* **12,** 1813–1821
63. Porter, J. D., Merriam, A. P., Leahy, P., Gong, B., Feuerman, J., Cheng, G., and Khanna, S. (2004) Temporal gene expression profiling of dystrophin-deficient (mdx) mouse diaphragm identifies conserved and muscle group-specific mechanisms in the pathogenesis of muscular dystrophy *Hum. Mol. Genet.* **13,** 257–269
64. Porter, J. D., Khanna, S., Kaminski, H. J., Rao, J. S., Merriam, A. P., Richmonds, C. R., Leahy, P., Li, J., Guo, W., and Andrade, F. H. (2002) A chronic inflammatory response dominates the skeletal muscle molecular signature in dystrophin-deficient mdx mice. *Hum. Mol. Genet.* **11,** 263–272
65. Greenberg, S. A., Sanoudou, D., Haslett, J. N., Kohane, I. S., Kunkel, L. M., Beggs, A. H., and Amato, A. A. (2002) Molecular profiles of inflammatory myopathies. *Neurology* **59,** 1170–1182
66. Tezak, Z., Hoffman, E. P., Lutz, J. L., Fedczyna, T. O., Stephan, D., Bremer, E. G., Krasnoselska-Riz, I., Kumar, A., and Pachman, L. M. (2002) Gene expression profiling in DQA1*0501+ children with untreated dermatomyositis: a novel model of pathogenesis. *J. Immunol.* **168,** 4154–4163
67. Yan, Z., Choi, S., Liu, X., Zhang, M., Schageman, J. J., Lee, S. Y., Hart, R., Lin, L., Thurmond, F. A., and Williams, R. S. (2003) Highly coordinated gene regulation in mouse skeletal muscle regeneration. *J. Biol. Chem.* **278,** 8826–8836
68. Paoni, N. F., Peale, F., Wang, F., Errett-Baroncini, C., Steinmetz, H., Toy, K., Bai, W., Williams, P. M., Bunting, S., Gerritsen, M. E., and Powell-Braxton, L. (2002) Time course of skeletal muscle repair and gene expression following acute hind limb ischemia in mice. *Physiol. Genomics* **11,** 263–272
69. Goetsch, S. C., Hawke, T. J., Gallardo, T. D., Richardson, J. A., and Garry, D. J. (2003) Transcriptional profiling and regulation of the extracellular matrix during muscle regeneration. *Physiol. Genomics* **14,** 261–271
70. Matecki, S., Guibinga, G. H., and Petrof, B. J. (2004) Regenerative capacity of the dystrophic (mdx) diaphragm after induced injury. *Am. J. Physiol.* **287,** R961–R968
71. Oexle, K., and Kohlschutter, A. (2001) Cause of progression in Duchenne muscular dystrophy: impaired differentiation more probable than replicative aging. *Neuropediatrics* **32,** 123–129
72. Conboy, I. M., Conboy, M. J., Smythe, G. M., and Rando, T. A. (2003) Notch-mediated restoration of regenerative potential to aged muscle. *Science* **302,** 1575–1577
73. Conboy, I. M., Conboy, M. J., Wagers, A. J., Girma, E. R., Weissman, I. L., and Rando, T. A. (2005) Rejuvenation of aged progenitor cells by exposure to a young systemic environment. *Nature* **433,** 760–764
74. Muntoni, F., Fisher, I., Morgan, J. E., and Abraham, D. (2002) Steroids in Duchenne muscular dystrophy: from clinical trials to genomic research. *Neuromuscul. Disord.* **12,** S162–S165
75. 't Hoen P. A., van der Wees C. G., Aartsma-Rus A., Turk R., Goyenvalle A., Danos O., Garcia L., van Ommen G. J., den Dunnen J. T., and van Deutekom J. C. (2006) Gene expression profiling to monitor therapeutic and adverse effects of antisense therapies for Duchenne muscular dystrophy. *Pharmacogenomics* **7,** 281–297
76. Balagopal, P., Olney, R., Darmaun, D., Mougey, E., Dokler, M., Sieck, G., and Hammond, D. (2006) Oxandrolone enhances skeletal muscle myosin synthesis and alters global gene expression profile in Duchenne muscular dystrophy. *Am. J. Physiol.* **290,** E530–E539

Received for publication September 15, 2006.
Accepted for publication November 21, 2006.